ChemComm

Accepted Manuscript

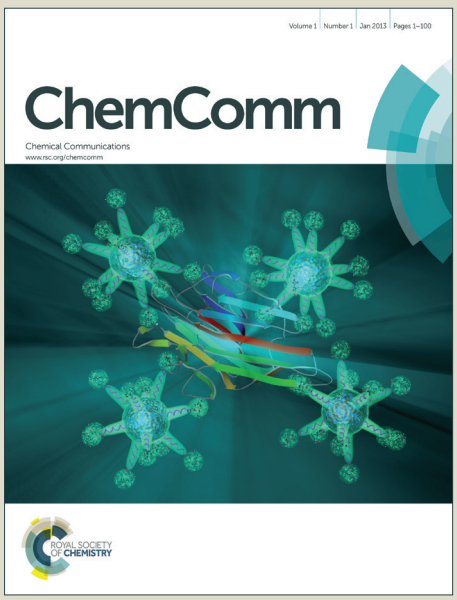

ROYAL SOCIETY OF CHEMISTRY

www.rsc.org/chemcomm

Chemical Communications RSCPublishing

COMMUNICATION

Design, Synthesis and Biological Evaluation of Mitochondria Targeted Theranostic Agents

Cite this: DOI: 10.1039/xoxxoooooox

Song Wu,[a,b] Qizhen Cao,[a] Xiaolin Wang,[a,c] Kai Cheng, Zhen Cheng[a*]

Dually mitochondrial targeted fluorescent F16-TPP analogues were designed and synthesized. The uptake and cytotoxity studies indicate that FF16 and FF16-TPP, the two compounds discovered in this study, are promising mitochondria targeted theranostic agents.

Mitochondria play significant roles in a variety of biological processes from cell life to death[1]. Mitochondria dysfunction are extensively involved in many types of human diseases[2] and thus prompts the research on mitochondria-specific diagnosis and therapies.[3] Tetraphenylphosphonium and its analogue alkyltriphenylphosphonium (TPP) salts are lipophilic cations that are able to cross mitochondria and accumulate within mitochondria matrix which are driven by high membrane potential (Scheme 1).[4] TPP analogues have been extensively used as mitochondria targeted carriers for biomedical applications by conjugating TPP and drugs covalently[5]. TPP analogues also play a significant role in mitochondria targeted imaging of diseases. For example, radionuclides such as ^{3}H, ^{18}F, ^{64}Cu, and ^{99m}Tc labelled TPP and its analogues, as well as fluorophore modified analogues, have been successfully used to study mitochondria-related events in cell and/or animal models.[6] With the fast advancement on understanding the biological role of mitochondria, it is expectable that TPP compounds would find more applications.

The demand for new therapeutics targeting to mitochondria prompts the discovery of new agents that can interfere physiological activities in mitochondria. A small molecule F16 (structure shown in Scheme 1) is one exemplary agent that shows interesting properties both on fluorescent imaging and therapy for cancers.[7] As a delocalized cationic (DLC) compound, F16 exhibits excellent optical properties with fluorescent emission at a visible region, and more interestingly, it shows mitochondria specific accumulations in a variety of cancer cell, thus resulting in cytotoxicity by triggering apoptosis and necrosis of the cells.[7]

A theranostic agent that combines diagnosis and therapy simultaneously is of great significance for clinical applications. Considering the specific mitochondria targeting ability of both TPP and F16, as well as the imaging ability and cytotoxicity activity toward various cancer cell lines of F16, coupling F16 analogues with TPP may provide novel agents for cancer imaging and treatment. Such potential theranostic agents may show the following advantages. First, TPP is a molecule which can't be imaged directly. Tedious and costly procedure is required to include radionuclides such as ^{18}F for visualization of diseased tissue.[6] Coupling TPP with F16 could thus provide TPP analogues with optical imaging and cytotoxic ability simultaneously. Such conjugates may find applications in cell mitochondria imaging and image guided surgery that needs good fluorescence contrast between cancer and normal tissues.[8] Second, since both F16 and TPP analogues possess mitochondrial targeting ability, coupling them together results in DCLs with two positive charges which can likely maintain the mitochondria targeting ability. The functions of F16-TPP analogues for mitochondria targeting are shown in Scheme 1. In this study, three F16-TPP analogues (F16-TPP, FF16-TPP and MeF16-TPP) bearing different substituents were therefore synthesized along with F16 and a F16 derivative (FF16) for comparison. The conjugates were synthesized in a way similar to F16 as shown in Scheme 2. The intermediate **6** was prepared by reacting 4-picoline and (4-bromobutyl)triphenylphosphonium bromide readily in ethyl acetate at a good yield of 72.4%. The following condensation of **6** and indole-3-carboxaldehyde analogues in methanol and purification with reverse HPLC thereafter gave the TPP-F16 derivatives yet at low yields (<15%). (see ESI for details).

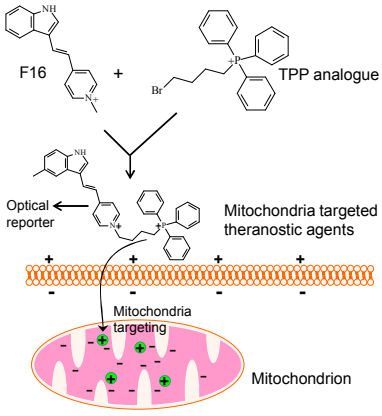

Scheme 1 Illustration of functions of F16-TPP conjugates.

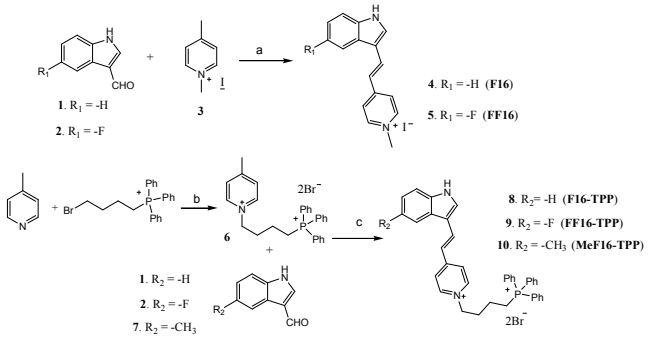

Scheme 2 Synthetic routes of F16 and F16-TPP analogues

Optical properties of all F16 related compounds were studied at a concentration of 5 μM in PBS buffer. As the spectra of the compounds shown in Figure 1a, all the compounds exhibited similar characteristics with close absorption and emission wavelengths for each other. The maximum absorption and emission are around 425 nm and 525 nm, respectively. Since TPP moiety is non-fluorescent, it is expected that F16-TPP conjugates inherit F16's optical characteristics. However, subtle influences of substituents on F16 and TPP moiety could be observed. For example, as shown in Figure 2a, both FF16-TPP and MeF16–TPP exhibited increasing fluorescence intensity at different levels in contrast to F16. Moreover, MeF16-TPP showed significant red shift of their absorption and emission wavelength compared to F16.

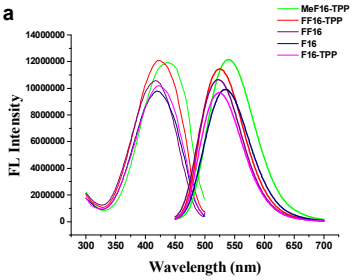

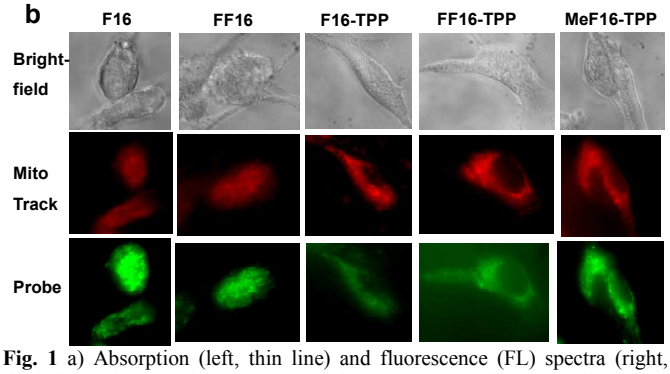

Fig. 1 a) Absorption (left, thin line) and fluorescence (FL) spectra (right, thick line) of F16 and F16-TPP related probes (5 μM) in PBS buffer (pH = 7.4). From the above to the bottom: MeF16-TPP (green). FF16-TPP (red); FF16 (purple); F16 (navy) and F16-TPP (magenta). b) The uptake of the F16 related probes in U87MG cells. From left to right column are brightfield, MitoTrack@, probe and overlay in each group, respectively. The FL intensity range for F16-TPP and FF16-TPP is 1000-2000, while for other probes is 2000-4000.

Tumor cell uptake of all F16 related compounds were studied by incubating two cancer cell lines (U87MG and MDA-MB-231) with the probes for 1 h and then imaged with a fluorescent microscope. Meanwhile, to investigate the localization of the F16 derivatives, after incubation with the probes, cells were co-stained with the commercially available dye Mitotrack@, which is widely used for mitochondria staining. The images of F16 related compounds in U87MG cells were displayed in Figure 1b. Under eGFP filter set (λex 450/490 nm, λem 515/565 nm), no significant autofluorescence of the cells were observed, making it convenient to study the relative uptake of the probes directly by comparing their fluorescence signals. Importantly, all compounds showed specific accumulations in the mitochondria of the tumor cells, which was proven by good overlay of images under the condition of the co-staining of the probes and Mitotrack@. These results demonstrate the mitochondria targeting ability of F16 analogues and F16-TPP conjugates.

We then investigated the uptake of all the probes in U87MG and MDA-MB-231 cells at 1 h incubation by quantitative analysis of fluorescent signals intensity of all F16 related compounds in the cells. The cellular uptake experiments were repeated nine times, and the relative cellular uptakes ability of different probes were calculated by comparing their percentage of cellular fluorescent signals and then normalized by that of F16 (Figure 2). For these probes, their uptake performance in U87MG and MDA-MB-231 was in generally quite similar. For instance, F16, FF16, F16-TPP and MeF16-TPP all showed similar uptakes in both cell lines ($P > 0.05$). Notably, only FF16-TPP displayed a dramatically increased uptake in MDA-MB-231 cells than that in U87MG ($P < 0.05$). Figure 2 also revealed the structural impact of the F16 related compounds towards their uptakes. For U87MG cells, F16, FF16 and MeF16-TPP all showed high and comparable uptakes (~1), while F16-TPP and FF16-TPP exhibited much lower uptakes than other probes (approximately half of the uptake of F16, $P < 0.05$). For MDA-MB-231 cell line, all F16 derivatives showed comparable uptakes except F16-TPP with about half uptake in contrast to the other probes.

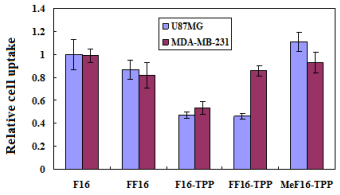

Fig. 2 The relative uptake of all F16 and F16-TPP analogues. The data was obtained by calculating by the following equation: Fluorescence signal in cell lines/ Fluorescence signal in PBS buffer and normalized to F16 in the U87MG cell line. n = 9. Data are presented as mean ± SD.

Apart from the imaging studies, we then investigated antitumor activities of all F16 related compounds by studying their antiproliferative effects in U87MG and MDA-MB-231 cell lines. After exposure of 5 or 10μM of the compounds in the cancer cells for 4 days, the cell proliferative ratios to the control were measured and showed in Figure 3. At a lower concentration of 5μM, all compounds exhibited no antiproliferative activities for U87MG cell line, while low to moderate activities with antiproliferative ratio less than 30% could be observed for MDA-MB-231 cell line (see Figure 3A). With increasing of concentration, the compounds showed distinct antitumor activities in two cell lines. As shown in Figure 3B, at a concentration of 10 μM, all the compounds prepared displayed

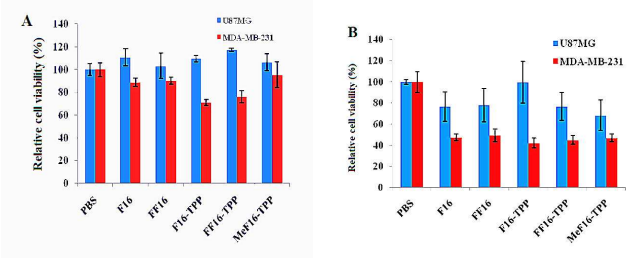

Fig. 3 Antiproliferative effect on the F16 and F16-TPP analogues. Data are expressed in cell proliferative ratio with exposure of the compounds for 4 days to the negative control in PBS buffer. [A] Cells were treated with 5 μM compounds. [B] Cells were treated with 10 μM compounds. n = 4. Data are presented as mean ± SD.

weak antitumor activities by their antiproliferative ratio less than 32% for U87MG cell line. However, as for MDA-MB-231 cell line, all compounds showed the much stronger cytotoxicity with a similar antiproliferative ratio over 50%. The different antiproliferative activities imply that the antitumor potency of the F16 related compounds is cell-dependent. Meanwhile, substituents in F16 and F16-TPP analogues played distinct roles, for instance, introduction of fluorine atom to F16 barely influences activity of FF16 ($P >$

0.05), while substituted fluorine and methyl group apparently impact F16-TPP analogues in U87MG cell line at a higher concentration of 10 μM.

To further confirm the relationship between cell uptake and antitumor activity, the half inhibitory concentrations (IC_{50}) of these compounds against U87MG cell line were measured. The IC_{50} for F16, FF16, F16-TPP, FF16-TPP and MeF16-TPP are 36.5±1.1, 28.0±1.2, >200, 28.9±1.1, and 64.0±1.3 μM, respectively (Supplemental file, Table 1, Figure S1). Interestingly, substitution of fluorine in F16 molecule slightly improve the bioactivity of the resulting compound (~1.3 fold), whereas adding a fluorine in F16-TPP dramatically improve the bioactivity of the resulting compound (>6.9 fold). Moreover, adding a methyl group to F16-TPP also improved its toxicity over 3 fold. It should be noted that all these five compounds show minimum or even un-observable toxicity in the fibroblast cell line NIH 3T3 (IC_{50} all >100 μM, Supplemental file, Table 1, Figure S1), highlighting the treatment specificity of these mitochondrial targeted agents.

Our cell imaging and treatment study confirm that F16-TPP analogues preserve the tumor cell mitochondria targeting ability and can be used for cancer cell fluorescence imaging and treatment. Especially, we successfully developed a theranostics agent FF16-TPP which showed fluorescence imaging ability and increased activity compared to F16. Meanwhile, we discovered that FF16 also showed superior cell killing ability compared to F16, demonstrating a simple fluorination of F16 can improve its anti-tumor activity while maintaining its optical properties.

One thing to note is that F16-TPP shows low cell uptake and killing ability, which is beyond with our initial expectation for synergistic effects that the conjugate should bring about. This may be ascribed to that the F16-TPPs bear more positive charges than F16 (2+ *vs.* 1+), which may lead to the reduced permeability of the conjugates into cells. While further substituting a lipophilic methyl group or electronegative fluorine atom to F16-TPP, MeF16-TPP and FF16-TPP show greatly enhanced cell killing capability (Figure 2, supplemental Table 1 and Figure S1). These data suggest the importance of fine tuning the structure of F16-TPP to achieve high cancer cell killing ability.

Since TPP itself does not impart cytotoxity as revealed by some studies,[9] it is reasonable to hypothesize F16-TPP conjugates kill tumor cells in a similar way as F16 by higher accumulation in tumor cells than in normal cells, which is caused by higher membrane potentials of mitochondria (ΔΨm) in tumor cells.[7] Indeed F16 and F16-TPP analogues all display much higher accumulations in U87MG cells than that in NIH 3T3 cells ($P < 0.05$, Supplemental file, Figure S2-S6). Apparently this cytotoxity is associated with accumulation level of the compounds. This may explain why F16 related compounds show higher antitumor activities at higher concentration of 10 μM than those at 5 μM. As for distinct cytotoxities of the same compound in different cell lines, these may be attributed to the distinct membrane potentials of mitochondria between the two cell lines we used. However, substituents like fluorine and methyl group exhibit negligible impacts on cytotoxities to MDA-MB-231 cell line at 10 μM, which are quite different from the uptake tendency shown in Figure 2. This may be caused by different time courses used for two studies (1 hour for cell uptake assay and 4 days for proliferation assay). Another possibility is that mitochondria accumulation may not be the only factor that influences the antiproliferative activities. Different total charges and charge distributions may also affect their capability on reducing ΔΨm to result in further biological cascade effects such as inhibition of mitochondria respiration and cell death. More work is needed to reveal the accurate inhibiting mechanism of F16 and F16-TPP related compounds which is uncertain so far.

Conclusions

The fluorescent mitochondria-specific agents F16 analogues and F16-TPP conjugates were successfully synthesized. Especially, FF16 and FF16-TPP show higher potency and comparable or increased mitochondria accumulation in tumor cell lines compared with F16, making them excellent candidates for mitochondria targeted optical imaging and treatment. Moreover, the structural modification of F16 related compounds shows high impacts on their cell uptake and antitumor activities. Our findings will not only benefit development of mitochondria-targeted theranostic agents based on TPP and F16, but also expand the usage of TPP as a mitochondria carrier.

This work was supported, in part, by the Office of Science (BER), U.S. Department of Energy (DE-SC0008397), and NIH *In vivo* Cellular Molecular Imaging Center (ICMIC) grant P50 CA114747.

Notes and references

a. Molecular Imaging Program at Stanford (MIPS), Bio-X Program, Department of Radiology, Stanford University, California, 94305-5344 Tel: 650-723-7866; Fax: 650-736-7925; E-mail: zcheng@stanford.edu.
b. School of Pharmaceutical Sciences, Wuhan University, Wuhan 430071, PR China.
c. Faculty of Forensic Medicine, Zhongshan School of Medicine, Sun Yat-sen University, Guangzhou, 510089, P.R. China
Electronic Supplementary Information (ESI) available: [Materials, experimental details, characterization data, biological assays]. See DOI: 10.1039/c000000x/

(1) N. Apostolova, A. Blas-Garcia, J. V. Esplgues, *Curr. Pharm. Des.,* 2011**,** **17**, 4047.
(2) S. J. Tabrizi, J. Workman, P. E.Hart, L. Mangiarini, A. Mahal, G. Bates, J. M. Cooper, A. H. Schapira, *Ann. Neurol*., 2000**,** **47**, 80; V. Gogvadze, *Curr. Pharm. Des.,* 2011, **17**, 4034.
(3) R. Rotem, A. Heyfets, O. Fingrut, D. Blickstein, M. Shaklai, E. Flescher, *Cancer Res*., 2005**,** **65**, 1984
(4) L. B. Chen, *Annu. Rev. Cell Biol.*, 1988**,** **4**, 155.
(5) T. A. Prime, F.H. Blaikie, C. Evans, S. M. Nadtochiy, A. M. James, C. C. Dahm, D. A. Vitturi, R. P. Patel, C. R. Hiley, I. Abakumova, R. Requejo, E. T. Chouchani, T. R. Hurd, J. F. Garvey, C. T. Taylor, P. S. Brookes, R. A. Smith, M.P. Murphy, *Proc. Natl. Acad. Sci. USA.,* 2009, **106**, 10764.
(6) J-J. Min, S. Biswal, C. Deroose, S. S. Gambhir, *J Nucl Med.,* 2004, **45**, 636.; Z. Cheng, R. C. Winant, S. S. Gambhir, *J. Nucl. Med.,* 2005, **46**, 878; G. S. Gurm, S. B. Danik, T. M. Shoup, S. Weise, K. Tarahashi, S. Laferrier, D. R. Elmaleh, H. Gewirtz, *JACC Cardiovasc Imaging.,* 2012, **5**, 285; D. Y. Kim, H. J. Kim, K. H. Yu, J. J. Min, *Bioconjug. Chem.,* 2012, **23**, 431.; I. Madar, H. Ravert, B. Nelkin, M. Abro, M. Pomper, R. Dannals, J. J. Frost, *Eur J Nucl Med Mol Imaging.,* 2007, **34**, 2057; J. Wang, C. T. Yang, Y. S. Kim, S. G. Sreerama, Q. Cao, Z. B. Li, Z. He, X. Chen, S. Liu, *J. Med. Chem.,* 2007, **50**, 5057; Y. S. Kim, C. T. Yang, J. Wang, L. Wang, Z. B. Li, X. Chen, S. Liu, *J. Med. Chem.,* 2008, **51**, 2971; S. Chalmers, S. T. Caldwell, C. Quin, T. A. Prime, A. M James, A. Cairns, M. P. Murphy, J. G. MacCarron, R. C. Hartley, *J. Am. Chem. Soc.,* 2012, **134**, 758; H. M. Cocheme, A. Logan, T. A. Prime, I. Abakumova, C. Quin, S. J. McQuaker, J. V. Patel, I. M. Fearnley, A. M. James, C. M. Porteous, R. A. Smith, R. C. Hartley, L. Partridge, M. P. Murphy, *Nat. Protoc.,* 2012, **7**, 946.
(7) V. R. Fantin, M. J. Berardi, L. Scorrano, S. J. Korsmeyer, P. Leader, *Cancer Cell.,* 2002, **2**, 29; V. R. Fantin, P. Leader, *Cancer Res.,* 2004, **64**, 329.
(8) S. Keereweer, J. F. Kerrebijin, P. A. van Driel, B. Xie, E. Kaijzek, T. A. Snoeks, I. Que, M. Hutteman, J. van der Vorst, J. S. Mieog, A. Vahrmeijer, C. H. van de Velde, R. Baatenburg de Jong, C. G. Lowiks, *Mol. Imaging Biol.,* 2011, **13**, 199.
(9) M. Millard, D. Pathania, Y. Shabaik, L. Taheri, J. Deng, N. Neamati, *Plos One.*, 2010, **5**, e13131.